

Quantization of a Free Particle Interacting Linearly with a Harmonic Oscillator

Thomas Mainiero

Department of Physics, California Institute of Technology, Pasadena, CA 91125, USA

Mason A. Porter

*Department of Physics and Center for the Physics of Information,
California Institute of Technology, Pasadena, CA 91125, USA*

We investigate the quantization of a free particle coupled linearly to a harmonic oscillator. This system provides an ideal framework for studying the quantization of mixed systems because its classical counterpart has clearly separated chaotic and regular regions. We detect signatures of chaos in the quantum system by investigating properties such as avoided level crossings of eigenvalues as functions of the strength and range of the interaction. We also study Husimi distributions to compare the quantum dynamics to phase portraits of its classical counterpart. These comparisons allow one to identify key signatures of the classically chaotic and regular portions in the quantum system. We use this model problem to examine the quantum signatures of mixed regular-chaotic dynamics and show, in particular, that the Husimi structure becomes mixed and delocalized as the classical dynamics becomes more chaotic.

PACS numbers:

PACS: 05.45.Mt, 05.45.a,

Keywords: Quantum Chaos, Mixed Dynamics, avoided level crossings, Husimi distributions

The study of quantum chaos entails the investigation of the quantization of classical Hamiltonian systems with chaotic dynamics. Typical classical Hamiltonians systems are neither fully integrable nor fully chaotic but instead possess mixed dynamics (divided phase space), with islands of stability situated in a chaotic sea. Rigorous mathematical investigations of such systems are notoriously difficult because different analytical methods have been developed for systems with fully regular or fully chaotic dynamics. Recently, several (non-generic) classical Hamiltonian systems with clearly separated regular and chaotic regions have been investigated. In this paper, we study the quantization of one such system, consisting of a free particle interacting linearly with a harmonic oscillator. Analogous to the insights obtained in a recent study of the classical system [14], the separation into regular and chaotic components also allows more precise investigations of the quantum system than is typically possible, making this an ideal example to achieve a better understanding of the quantization of mixed systems. By examining avoided level crossings and Husimi distributions in the quantum system, we investigate the quantum signatures of mixed dynamics, demonstrating that the Husimi structures of nearby states become mixed and delocalized as chaos becomes a more prevalent feature in the classical phase space.

INTRODUCTION

Two major 20th century discoveries transformed scientists' understanding of nonlinear phenomena. Kolmogorov-Arnold-Moser (KAM) theory demonstrated the stability of regular dynamics for small perturbations of Hamiltonian systems [3, 4, 28, 31] and the theory of stochasticity of dynamical systems (so-called "chaos theory") demonstrated the stability of strongly irregular dynamics under small perturbations [2, 39, 40].

Studying the quantization of chaotic systems, which has been prevalent for over thirty years [13, 19, 20, 21, 35], has become increasingly important as physicists conduct ever more experiments at small scales and design ever more devices that exploit the physics at such scales. For example, quantum chaos is known to be relevant in quantum dots [30] and Bose-Einstein condensates [49]. Experiments on quantum chaos, which have been conducted using microwave cavities [29, 42, 43], atom optics [1, 16], and other systems, have investigated phenomena that are both fundamental and diverse—ranging from the decay of quantum correlations [1] to localization in quantum wave functions [29] and chaotic scattering [30]. However, despite this wealth of research, it is still not entirely clear how to understand the notion of chaos in quantum mechanics. Quantum wave functions satisfy a linear differential equation (the Schrödinger equation), so sensitive dependence on initial conditions and the exponential divergence of nearby trajectories—key components for defining classical chaos—cannot be used to define quantum chaos. Nevertheless, identifying features of

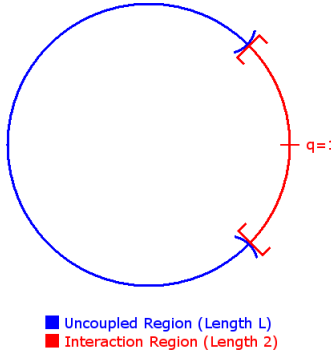


FIG. 1: [Color online] The configuration space of the particle. Its position on the ring is denoted q .

quantum analogs of classically chaotic systems do exist, so the quantizations of chaotic systems can be distinguished from the quantizations of integrable (regular) ones. The study of such identifying features using carefully chosen examples enables one to better understand the manifestations of chaos in quantum systems.

In the present paper, we investigate the quantization of a free particle interacting linearly with a harmonic oscillator, a recently-studied system with “mixed” dynamics (i.e., a divided phase space) which has well-separated integrable and chaotic regions [14]. In choosing this example, we are motivated by the fact that typical classical Hamiltonian systems are neither fully chaotic nor fully regular. Rather, they have mixed dynamics, with islands of stability (“KAM islands”) situated in a chaotic sea. Rigorous mathematical investigations of mixed systems are notoriously difficult because different analytical methods have been developed for systems with fully regular or fully chaotic dynamics and both approaches fail at the boundaries between chaotic and regular regions. Numerical investigations of systems with mixed dynamics are similarly difficult. Consequently, there have been numerous attempts to construct Hamiltonian systems with mixed dynamics that allow an exact, rigorous analysis. In addition to the aforementioned system, examples include billiards shaped like ovals [7], non-concentric circles [36], and mushrooms [6, 8, 33].

The rest of this paper is organized as follows. First, we briefly review the classical system studied in [14] that consists of a one-dimensional free particle interacting linearly with a one-dimensional harmonic oscillator. We then quantize this system and examine its sharp and broad avoided level crossings as the length of the interaction region is varied. We illustrate our observations using Husimi distributions, which also allow a comparison with the classical dynamics. Finally, we summarize our results and present additional technical details of our investigation in two appendices.

THE CLASSICAL SYSTEM

The interaction of two of the simplest quantum systems, the one-dimensional free-particle and the one-dimensional harmonic oscillator, arises in studies of dissipation in Hamiltonian systems [9] and electron-phonon interactions in solids [15, 17, 23, 24, 26, 38]. In condensed matter physics, in particular, there have been numerous theoretical studies of the rich dynamics of electron-phonon interactions, such as the emergence of “polaronic” quasi-particles. For example, in one version of T. Holstein’s molecular crystal model [23, 24], a tight-binding electron in a crystal moves between different sites, interacting with a local oscillator in each. Even the simplest “spin-boson” version of this model, which contains just two sites and one collective oscillator, cannot be solved exactly and has been the subject of intricate semiclassical investigations [27].

Recently, De Bièvre, Parris, and Silvius analyzed a simplified classical counterpart of such systems [14]. They considered a classical particle of mass m , position $x(t)$, and momentum $p_0(t)$ moving on a ring divided into two sections (see Fig. 1). In one section (of length L), the particle is free; in the other (of length $2σ$), it interacts with a harmonic oscillator of mass M , position $X(t)$, momentum $P(t)$, and frequency $ω$. The system’s Hamiltonian is

$$H = \frac{p_0^2}{2m} + \frac{P^2}{2M} + \frac{1}{2}M\omega^2X^2 - F_0X\rho(x), \quad (1)$$

where F_0 describes the strength of the interaction (which is linear in X). The quantity $\rho(x)$ determines the range of the interaction. It equals 1 when $|x| \leq σ$ and 0 when $|x| \in (\sigma, \sigma + \frac{L}{2})$, where we note that x is periodic (so that

$\sigma + L/2$ is identified with $-\sigma$). In non-dimensional form, Eq. (1) becomes

$$H = \frac{1}{2} (p^2 + \Pi^2 + \Phi^2) - \alpha \Phi \chi(q), \quad (2)$$

where p and Π are, respectively, the particle and oscillator momenta, q and Φ are the particle and oscillator positions, α describes the strength of the particle-oscillator interaction, and $\chi(q)$ is a function taking the value 1 in the interaction region and 0 everywhere else. The interaction and uncoupled (non-interaction) regions occur, respectively, when $q \in [-1, 1]$ and $q \in (1, 1+L)$, where L is the length of the uncoupled region and $1+L$ is identified with -1 . The only system parameters that can be varied are α and L . For convenience (for our subsequent analysis of the quantum system), we perform a simple coordinate transformation $q \mapsto q+1$, which leaves the form (2) invariant if $\chi(q)$ is redefined appropriately.

The equations of motion resulting from (2) and the subsequent coordinate transformation are

$$\begin{aligned} \dot{q} &= p, & \dot{p} &= \alpha \Phi [\delta(q) - \delta(q-2)], \\ \dot{\Phi} &= \Pi, & \dot{\Pi} &= -\Phi + \alpha \chi(q), \end{aligned} \quad (3)$$

where dots denote time derivatives. Equation (3) indicates that the particle behaves freely in both the interaction and non-interaction regions. The interesting dynamics of Eq. (3) arise because of what happens when a particle arrives at boundaries between the two regions (i.e., when $q = 0$ and $q = 2$; see Fig. 1). At these locations, the particle reaches a potential barrier of height $\pm \alpha \Phi$, where the sign depends on whether the particle is coming from the interaction region (+) or the non-interaction region (-). The particle bounces off the boundary elastically if its kinetic energy p^2 is less than the barrier height. Otherwise, it overcomes the barrier and enters the new region with a kinetic energy of $p^2 \mp \alpha \Phi$. Because the barrier height depends on the oscillator coordinate Φ , the dynamics can be rather complicated.

A particularly interesting facet of this system is the separation of the integrable and chaotic regions in its phase space. Phase portraits of the system possess two characteristic integrable regions (among other structures). The first, which exists for system energies varying from the ground-state energy $E_g = -F_0^2/(2M\omega^2)$ to a critical positive energy $E_c = |E_g|$, arises as a result of the particle never leaving the interaction area. For small positive energies outside this integrable region, the motion appears to be fully chaotic without any additional KAM structures near the boundary between the two regions [14]. The second integrable region is an elliptic KAM island centered on the equilibrium point that arises from the orbit in which the particle traverses each section of the ring exactly once per period. The distinction between chaotic and integrable dynamics is clear in a variety of situations in which one or both regions exist. This helps simplify comparisons between the dynamics of the classical system and its quantization and makes the present example a very illuminating one for studying the quantization of systems with mixed dynamics. The investigation of such correspondences is extremely difficult for generic mixed systems, which possess an infinite hierarchy of KAM islands and intricately mixed chaotic and integrable regions.

THE QUANTUM SYSTEM

We quantize Eq. (2) using canonical quantization [12]. In so doing, we assume the particle and oscillator act as bosons with no internal degrees-of-freedom and impose the following commutation relations:

$$[p, q] = i, \quad [p, \Pi] = 0, \quad [\Pi, \Phi] = i, \quad [q, \Phi] = 0, \quad [p, \phi] = 0, \quad [\Pi, q] = 0. \quad (4)$$

With the coordinate-space identifications

$$p = -i \frac{\partial}{\partial q}, \quad \Pi = -i \frac{\partial}{\partial \Phi}, \quad (5)$$

we then obtain the quantum Hamiltonian

$$H = \frac{1}{2} \left(-\frac{\partial^2}{\partial q^2} - \frac{\partial^2}{\partial \Phi^2} + \Phi^2 \right) - \alpha \Phi \chi(q). \quad (6)$$

For the uncoupled case ($\alpha = 0$), the time-independent Schrödinger equation $H|\psi\rangle = E|\psi\rangle$ is separable, so one just needs to determine the eigenstates of the harmonic oscillator and the free particle confined to a ring of length $2+L$ as separate problems (both of which admit closed-form solutions). Let $\{|\psi_{k+1}^{part}\rangle\}_{k=0}^{\infty}$ and $\{|\psi_l^{osc}\rangle\}_{l=0}^{\infty}$ denote

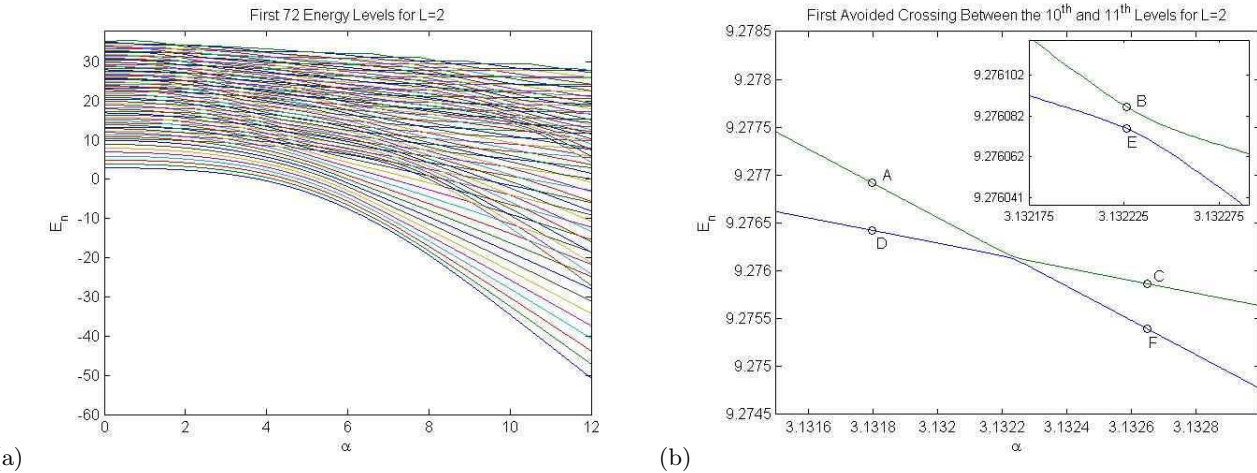


FIG. 2: [Color online] (a) The first 72 energy levels as a function of the interaction strength α for Eq. (6) with an uncoupled region of length $L = 2$. (b) Magnification of an avoided crossing between the 13th and 14th levels. The inset shows a further magnification. The labels designate where we calculated Husimi distributions (see Fig. 8a).

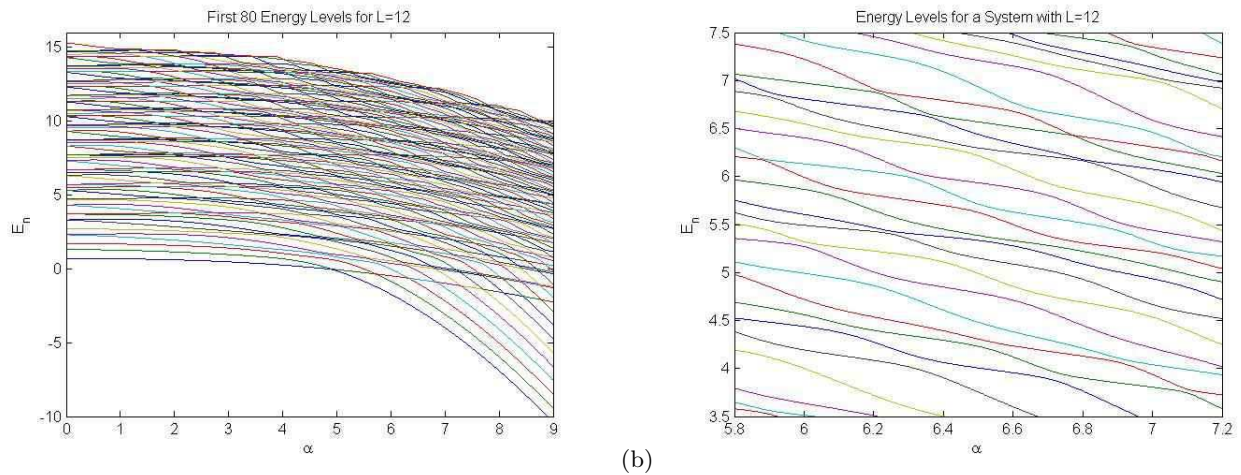


FIG. 3: [Color online] (a) The first 80 energy levels as a function of α for Eq. (6) with an uncoupled region of length $L = 12$. (b) Magnification of (a) illustrating broad avoided crossings.

eigenstates of the particle and the harmonic oscillator, respectively, so that $\{|\psi_{k+1}^{part}\rangle \otimes |\psi_l^{osc}\rangle\}_{k,l=0}^\infty$ are eigenstates for the uncoupled system [52]. In fact, these states form a basis for the Hilbert space of either the coupled or uncoupled system. We represent the Hamiltonian (6) as an infinite matrix using this basis (see Appendix I) and approximate its eigenvalues and eigenstates using those of a truncation of the matrix.

AVOIDED CROSSINGS

As the coupling parameter α is varied, the eigenvalues of (6) can approach each other very closely or even cross. If the Hamiltonian is invariant under a symmetry transformation [53] for a certain range of α , it can be block-diagonalized by exploiting this symmetry. We do this by choosing each block to be invariant under the symmetry transformation. Energy levels belonging to different blocks can cross as α is varied [21, 35, 47]. On the other hand, if a quantum Hamiltonian has no symmetries other than time reversal, then such a level crossing is called an “accidental degeneracy” and requires the confluence of two parameters [35]. In this case, most levels that approach each other end up avoiding one another instead of crossing.

Classically chaotic systems have fewer constants of motion than degrees-of-freedom and thus have fewer symmetries than integrable systems with the same number of degrees-of-freedom. One expects the quantization of these two

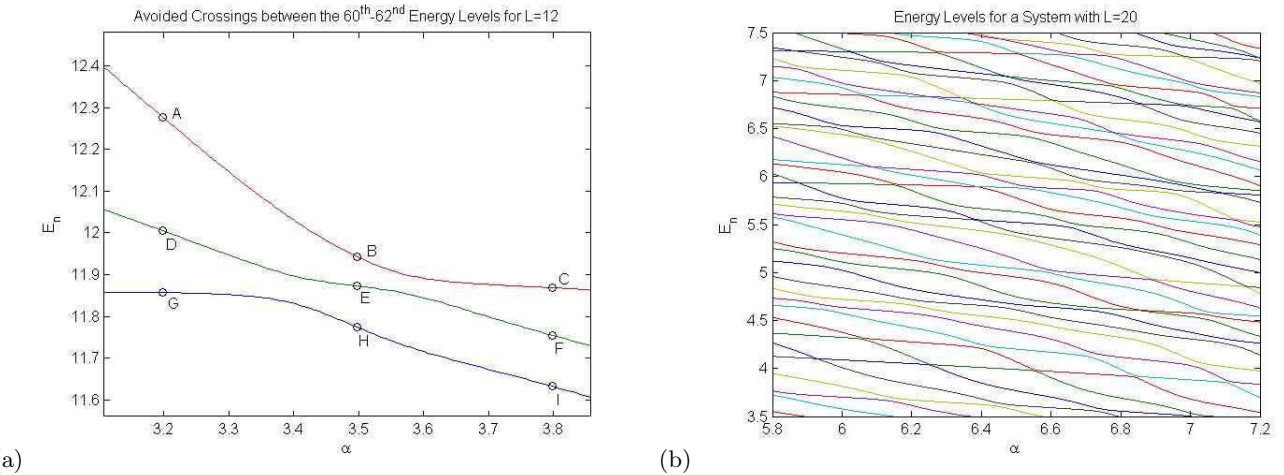


FIG. 4: [Color online] (a) A nearly isolated cluster of broad avoided crossings between the 60th, 61st, and 62nd levels for $L = 12$. The dynamics of the 60th level is influenced slightly by the 59th, and the incoming slope of the 60th level is imparted to the outgoing slope of the 62nd. The labels designate locations at which we calculated Husimi distributions (see Fig. 8b). (b) Broad avoided crossings between levels for a system with $L = 20$. Note the increased density of energy levels and avoided crossings compared to Fig. 3b.

situations to exhibit signatures of this difference [50, 51]. Hence, the quantization of a chaotic system should possess fewer level crossings than the quantization of an integrable one and the presence of numerous avoided crossings between energy levels may be a signature of chaotic regions in the classical system. Indeed, avoided level crossings are typical features of quantum chaotic systems [18, 25, 34, 46, 48].

Figure 2a shows the first 72 energy levels as a function of α in a system with $L = 2$ using an α -step size of 2.5×10^{-3} and a 2025×2025 truncated Hamiltonian matrix. (The α -step size is the distance between successive values of α for which we calculate eigenvalues and eigenvectors.) One observes a multitude of apparent level crossings. Refining the numerical computation at some of these apparent crossings shows that they are actually avoided crossings in which the slopes of the energy level curves are exchanged. Avoided crossings of this nature are known as “sharp” avoided crossings [35, 46]. In passing through such avoided crossings, the participating levels exchange their eigenstate structures, behaving as though they had entered a level crossing [47]. As we discuss in more detail later, we have verified numerically that this indeed occurs for our system. Similar phenomena have also been observed in other systems, such as a sinusoidally driven particle in a square potential well [46] and a hydrogen atom in a strong magnetic field [18].

Figure 2b shows a magnification of an avoided crossing between the 13th and 14th levels in Fig. 2a using a refined α -step size of 2×10^{-6} . In general, the α -step size at which the avoided crossings in Fig. 2b can be resolved is $O(10^{-6})$. As a result, it is time-consuming to verify numerically that all of the apparent crossings are actually very sharp avoided crossings. However, the coupled Hamiltonian possesses no physically obvious symmetries other than time-reversal. (All symmetries of the uncoupled Hamiltonian have been broken; there is no parity and $[H, p] \neq 0$ for $\alpha \neq 0$.) Assuming this is true, level crossings would constitute accidental degeneracies, which are rare (as discussed previously). Rigorously proving the Hamiltonian has no other symmetries is a difficult problem in general.

Another notable feature of Fig. 2a is that the first nine energy-level curves are much more widely spaced than higher energy-level curves and have a much lower frequency of avoided crossings as α is varied. The first nine energy-level curves accordingly oscillate much less as a function of α than do the higher energy levels. This is unsurprising, as in the uncoupled system with $L = 2$, the first nine levels of the oscillator all have a lower energy than that of the ground state of the particle. This gives the levels of the system their wide spacing, which is preserved as α increases. The wide spacing prevents close encounters between these levels, in contrast to what happens for higher-energy levels. As L increases, however, the ground-state energy of the particle drops quadratically in L and one does not expect this behavior to hold.

Figure 3a shows the first 80 energy-level curves for $L = 12$. Our numerical computations, for which we used a 5625×5625 truncated Hamiltonian matrix, verify that the frequency of avoided crossings in the first few levels increases as L grows. Even more interesting are the broad avoided crossings, which become more prevalent as α increases. Figure 3b shows energy-level curves for $\alpha \in [5.8, 7.2]$. The α -step size for which the sharp avoided crossings in this figure can be resolved is $O(10^{-3})$, about one thousand times larger than that required to resolve the

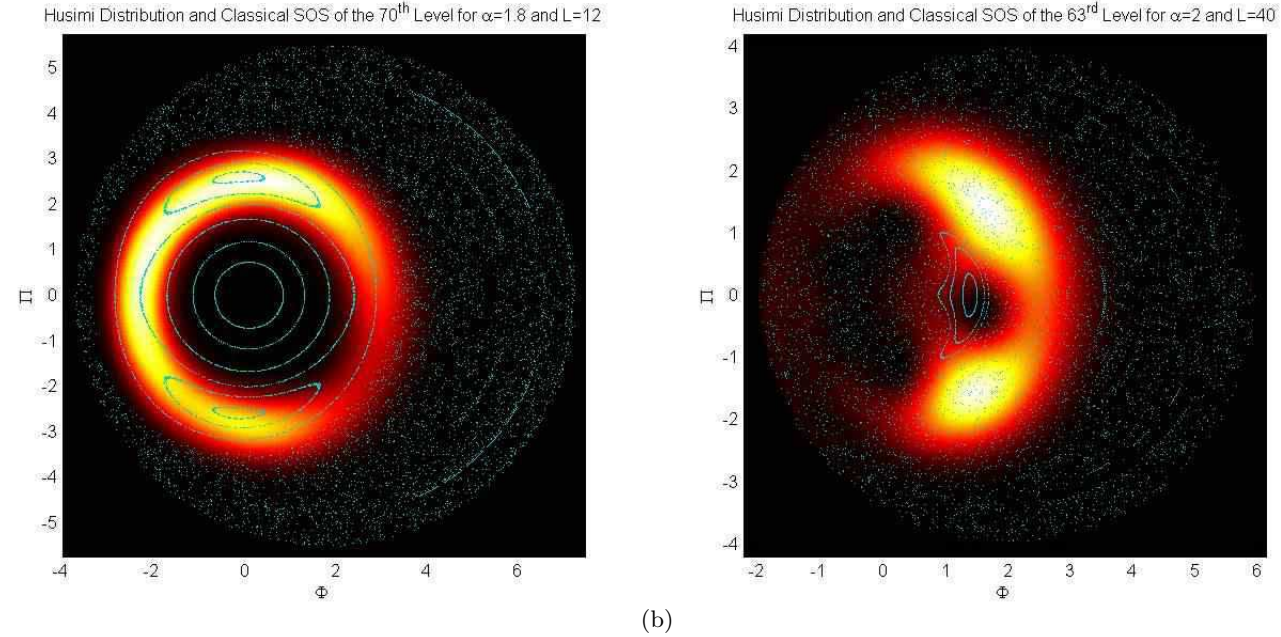


FIG. 5: [Color online] (a) Husimi distribution showing strong anti-scarring, as it localizes around the KAM island in the classical phase space. Lighter regions of the Husimi distribution have higher probabilities and black regions are ones in which the Husimi distribution vanishes. The classical SOS is plotted in turquoise. To facilitate the comparison between the quantum and classical dynamics, we include plots of a few of the orbits in the integrable region. (b) Husimi distribution localized *near* (rather than on) the KAM island but having the same shape. We again plot a few of the orbits in the integrable region.

sharp avoided crossings in Fig. 2a. The broad avoided crossings tend to occur in nearly isolated clusters in which only a subset of the initial slopes of the participating levels are exchanged after the sequence of crossings in the cluster [54]. Hence, one would not necessarily expect a complete exchange of eigenstate structure for these avoided crossings. Indeed, prior work on a sinusoidally driven particle in a square potential well shows a superposition of eigenstate structure in broad avoided crossings rather than a complete exchange [46]. We will use the term “mixing” to refer to such a superposition. An example of an isolated cluster of avoided crossings is shown in Fig. 4a.

Figure 4b shows the energy-level curves for a system with $L = 20$ using the same window as in Fig. 3b. Because of the increased density of energy levels and the larger number of broad avoided crossings, it is more likely that broad crossings occur in clusters in which the slopes are not completely exchanged. The ground-state energy of the free particle is proportional to $1/(2 + L)^2$, so the density of levels in the ground state should increase with L . Consequently, as long as this increased density is roughly preserved with α (which seems to hold in our numerical computations), then one would expect more broad avoided crossings with increasing L .

HUSIMI DISTRIBUTIONS

Although there is no equivalent of classical phase space trajectories in quantum mechanics, there are suitable analogs. In particular, the Husimi distribution is often used in the study of quantum chaos [19]. Given a quantum state $|\psi\rangle$, its Husimi distribution $H_\psi(p, q)$ is defined by the projection of $|\psi\rangle$ onto a coherent state $|\psi_{(p,q)}\rangle$ localized around (p, q) so that $H_\psi(p, q) \propto |\langle\psi_{(p,q)}|\psi\rangle|^2$. For a system with a Euclidean topology, a coherent state localized at (p, q) is a Gaussian, with position-space representation localized around q and momentum-space representation localized around p . The present system possesses a cylindrical phase space topology, as the particle position q is a periodic variable and the momentum $p \in \mathbb{R}$. In Appendix II, we construct the coherent state for this topology from the Euclidean coherent state [41].

Coherent states provide excellent quantum analogs of classical particles when visualized as wave packets that minimize the position-momentum uncertainty product. The projection onto these particle-like states can thus be viewed intuitively as a sort of classical smearing. One then interprets the Husimi distribution as a probability distribution in phase space [5], so that it provides a quantum analog of a phase portrait. See [5, 10, 11, 32] for

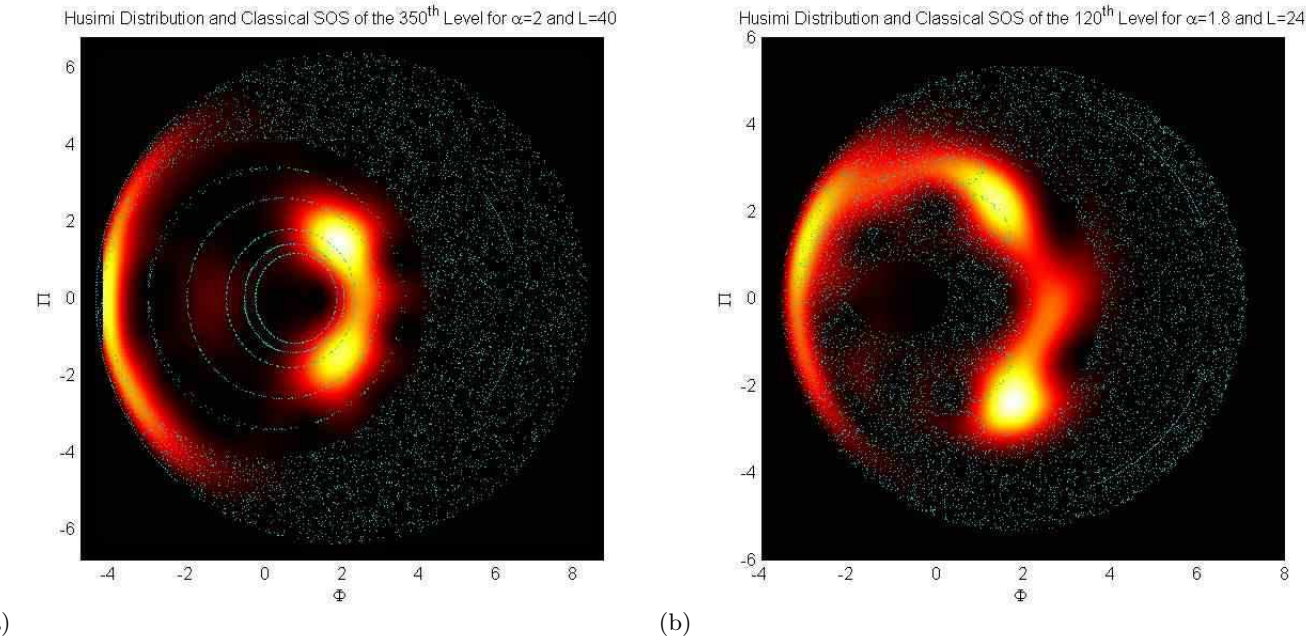


FIG. 6: [Color online] (a) Anti-scarring and strong localization in the chaotic region (along the periphery of the plot). (b) Husimi distribution showing both chaotic and integrable features while clearly having only one connected component.

additional discussion and applications. In the classical system (2), we view the oscillator phase space $[(\Phi, \Pi)\text{-space}]$ as classical Poincaré surfaces of section (SOS) taken at $q = 1$ and $p > 0$ [14]. On this same section, we calculate Husimi distributions in the quantum oscillator phase space for eigenstates of the Hamiltonian (6) (see the discussion in Appendix II). Using the eigenstate energy and the same system parameter (α and L) values, we compare the Husimi distributions to corresponding classical SOS.

Localization Around Classical Features

To investigate the signatures of chaotic and integrable dynamics on a quantum system, one can compare the quantum Husimi structure to corresponding classical Poincaré sections [5, 32, 46]. One manifestation is scarring (anti-scarring), in which an eigenstate tends to localize around unstable (stable) periodic orbits [19].

We have found anti-scarring to be extremely prevalent in the eigenstates of Eq. (6). For example, Fig. 5a shows an anti-scared state in which the Husimi structure is strongly localized in the integrable region of the classical SOS. We display the Husimi distribution as a contour plot that varies from black (zero probability) to white (about 10^{-3}), with lighter regions having higher probability than darker regions. We overlay the classical SOS in turquoise. We observe that the quantum manifestation of a classical integrable region (a KAM island) is a Husimi structure strongly localized inside the region. By analogy with the classical dynamics, we refer to such states as “regular.” We also observed states that were not as clearly localized in integrable regions but were instead localized in nearby regions possessing the same characteristic shape (see, for example, Fig. 5b).

Figure 6 also shows anti-scarring, along with the equally prevalent structure of strong localization in the chaotic sea of the associated classical SOS (particularly around the edge on the left half of the SOS). By analogy with the classical dynamics, we refer to quantum states with only the latter structure as “chaotic.” This structure persists even for large energies for which the chaotic region in the left half of the SOS retreats to the edge of the available phase space, as illustrated in Fig. 6a. In our computations, we have only observed Husimi structure localized around the left half of the available phase space. This may be due to continuity of the Husimi distribution as the particle position \bar{q} (see Appendix II) is varied from the non-interaction region of phase space to the interaction region in which our classical SOS are taken. The (disk-shaped) non-interaction region in phase space partially intersects the left half of the classical SOS for the majority of eigenenergies in the parameter ranges we studied (we varied the uncoupled length L from 2 to 40). [14]. When L is larger, the system’s ground state has a lower energy and a higher density of states. More complex features (i.e., hierarchies KAM islands throughout the phase space) sometimes exist for these

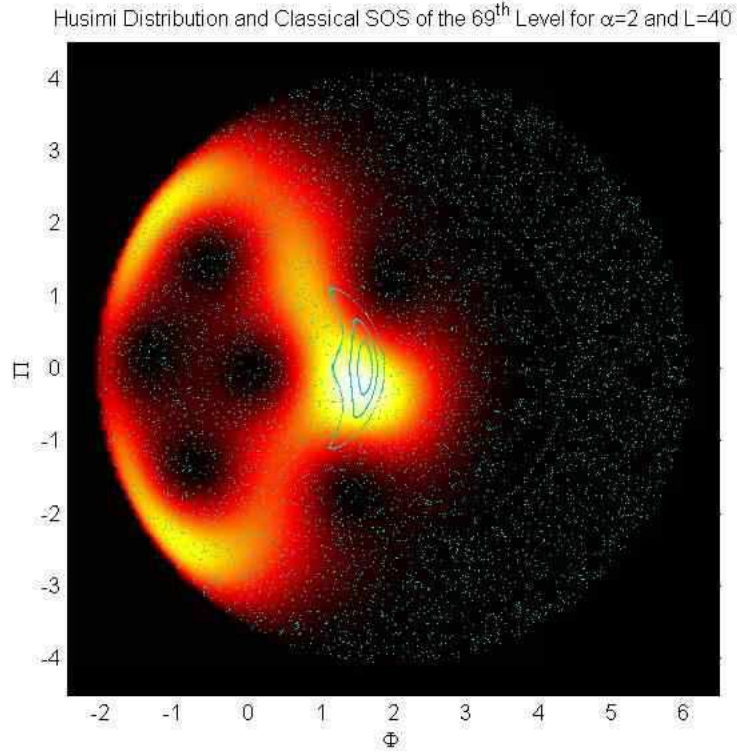


FIG. 7: [Color online] Husimi distribution showing both chaotic and integrable features while having only one connected component. The plot is relatively delocalized throughout the enclosed area on the left side of the available phase space. We also show a few of the orbits in the integrable region.

lower energies and one might concomitantly observe a more complicated Husimi structure.

Figures 6b and 7 provide examples containing a strong mixture of regular and chaotic Husimi structures (which here consist clearly of one connected component). The “bridge” that is often observed between integrable and chaotic regions serves as a channel through which Husimi structure continuously flows between regions as α is varied through an avoided crossing. We did not observe any Husimi distributions in which the regular and chaotic components were completely disconnected. The regular and chaotic components of Fig. 6a may seem disconnected at first glance, but one can see upon closer inspection that they are actually connected by small bridges of non-zero Husimi probability. Another interesting feature is the delocalized appearance of Fig. 7 in comparison to most of the Husimi distributions we computed: Husimi probability seems to be distributed throughout the region contained inside the bridges between the integrable and chaotic regions. This is a signature of the predominantly chaotic dynamics of the classical SOS.

Exchange and Mixing of Husimi Structure at Avoided Crossings

Sharp Avoided Crossings

In Fig. 8a, we depict the Husimi distributions for the 10th and 11th energy levels (with $L = 2$), with corresponding classical SOS overlaid. This plot reveals the structural changes as the two levels encounter the avoided crossing in Fig. 2b. In the top panels, we see that the 10th level is a regular state, whereas the 11th level is chaotic. The middle panels are snapshots near the closest point of the encounter. Here, the distributions appear as mixtures of the two initial Husimi distributions. Additionally, the regular and chaotic portions of the structure are connected and – as α is varied – Husimi probability flows continuously between integrable and chaotic regions. The bottom panels, depicting snapshots from long after the encounter, show that the two levels have completely exchanged their structure through the avoided crossing, leaving the aggregate Husimi structure unchanged. This provides an example of a smooth exchange of character in a sharp avoided crossing, which has also been observed in other quantum chaotic

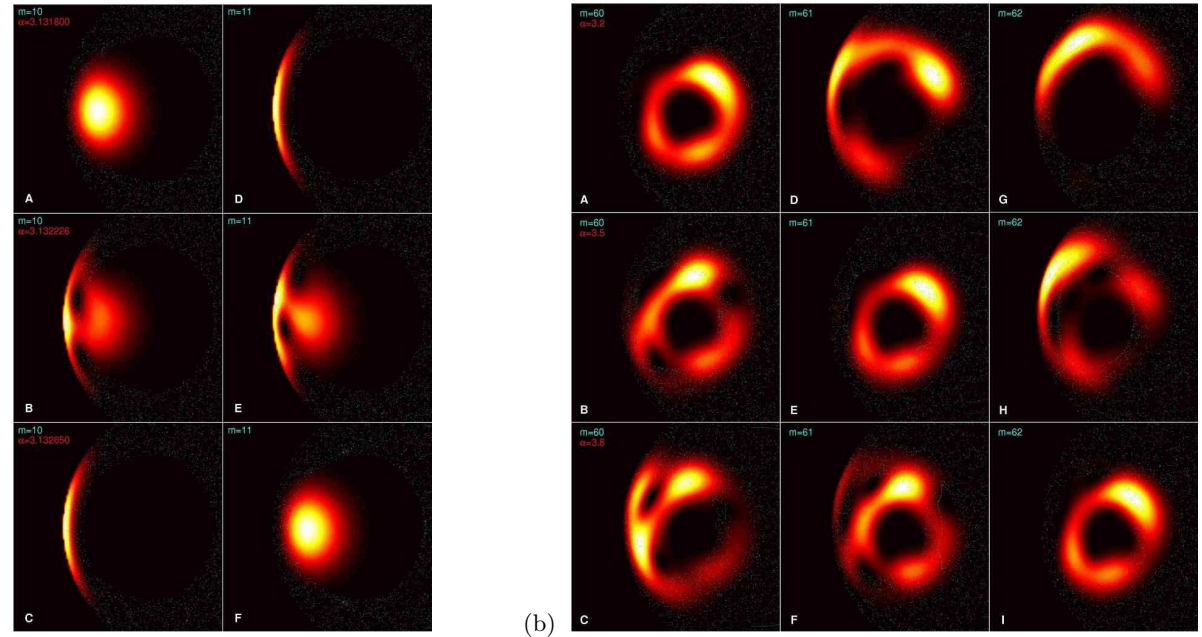


FIG. 8: [Color online] (a) Husimi structure exchange through the sharp avoided crossing shown in Fig. 2b. (As before, lighter regions have higher probabilities.) The left and right columns are the Husimi distributions of the 10th and 11th levels, respectively. The variable Π is on the vertical axis and Φ is on the horizontal axis. The corresponding classical SOS are overlaid in turquoise. During the structure exchange, probability flows continuously from the integrable region to the chaotic region for the 10th eigenstate (and vice-versa for the 11th). (b) Mixing of Husimi structures through the broad avoided crossings of Fig. 4a. The left, middle, and right columns show the Husimi distributions of the 60th, 61st, and 62nd levels, respectively.

systems [22, 46]. Thus far, the only avoided crossings between chaotic and regular states that we have observed have been sharp ones.

Broad Avoided Crossings

As described previously, the energy-level curves in broad avoided crossings typically occur in nearly isolated clusters in which the initial slopes of the curves are not fully exchanged after the sequence of avoided crossings. This typically leads to a “mixing” of Husimi structures rather than a complete exchange [46], which we have verified is the case for the Hamiltonian (6). For example, Fig. 8b shows such a mixing in the cluster of avoided crossings from the 60th through the 62nd energy levels from Fig. 4a. The localization of the initial Husimi structure of the 60th level indicates that this eigenstate is regular. The 61st level is localized mainly near an integrable region with a significant chaotic localization, and the opposite behavior is observed for the 62nd. The 60th and 61st levels leave the avoided-crossing cluster with Husimi structures that appear as mixtures between the initial Husimi structures of the 61st and 62nd levels. The 62nd state, however, leaves with a Husimi structure nearly identical to the initial structure of the 60th state. These observations are consistent with the slope exchanges in Fig. 4a. This mixing causes the Husimi distributions of the 60th and 61st levels to delocalize after the avoided-crossing cluster. Thus, in contrast to sharp avoided crossings, broad avoided-crossing clusters play a significant role in modifying the aggregate Husimi structure as the coupling strength α increases. In particular, such clusters appear to mix and delocalize the Husimi structure of individual eigenstates. Because broad avoided crossings become increasingly prominent (as compared to sharp avoided crossings) for larger L , one expects the aggregate Husimi structure to depend more strongly on the coupling strength α as L is increased (i.e., as the non-interaction region becomes larger).

Localization and Scale of Avoided Crossings

Our observations show qualitatively that the resolution of an avoided crossing (that is, the α -step size required to resolve the crossing) is correlated with the initial localization in the Husimi structures of the participating energy

levels. For the non-interaction length $L = 2$, Husimi distributions have a strong chaotic or regular identity, as they are almost completely localized in one of the two types of regions. This system's avoided crossings can be resolved by α -step sizes $O(10^{-6})$. As L is increased, the α -step size at which even the sharpest avoided crossings can be resolved tends also to increase. We have observed that the sharp avoided crossings involve an interaction between a level localized primarily in an integrable region (with only slight localization with the chaotic region) and one localized primarily in a chaotic region (with only slight localization with the integrable region). On the other hand, broad avoided crossings such as those in Fig. 4a tend to involve interactions between levels with significant localization in both integrable and chaotic regions. Adjacent eigenstates that are both localized predominantly in an integrable region (or chaotic region) tend to have nearly parallel energy-level curves (as a function of α). For example, the 60th and 61st energy-levels curves in Fig. 4a are nearly parallel after the broad avoided crossing and are predominately localized in the integrable region (see panels F and I of Fig. 8b). The α -step size at which an avoided crossing can be resolved seems to decrease (increase) as the localization of the participating levels in different (similar) regions of the classical SOS increases (decreases). Because broad avoided-crossing clusters tend to delocalize and mix the Husimi structure of the participating levels, this helps explain why broad avoided crossings seem to become more prominent as α is increased (see, e.g., Fig. 3a). One can investigate this phenomenon quantitatively by comparing the resolution of avoided crossings with quantitative measures of localization [21], thereby obtaining a quantitative distinction between sharp and broad avoided crossings and establishing additional connections to the classical dynamics.

Signatures of Chaos

As ergodicity and exponential divergence of phase-space trajectories can be used to characterize classically chaotic systems, it has been suggested that delocalization in the Husimi distributions of a quantum system is a possible signature of chaos in its classical counterpart [44]. This has been quantified and studied in numerical investigations [45, 46] and is also germane to the system investigated here, as the fraction of phase space with chaotic dynamics in the classical system (2) increases with L [14]. Consequently, the delocalization and mixing of Husimi structures, which become more prominent as the prevalence of broad avoided crossings increases with L , seem to be signatures of the chaos in the corresponding classical system.

CONCLUSIONS

In this paper, we investigated the quantization of a model system with mixed regular and chaotic dynamics: a one-dimensional free particle on a ring coupled to a one-dimensional harmonic oscillator. By examining its eigenenergies as a function of the system parameters (coupling strength and the size of the uncoupled region) and computing Husimi distributions, we studied the quantum signatures of the mixed dynamics.

We identified key integrable, chaotic, and mixed structures of Husimi distributions by comparing them with their corresponding classical surfaces of section. With these identifications, we observed that sharp avoided crossings occur between states localized in chaotic regions and those localized in integrable ones and demonstrated numerically the concomitant complete exchange of the Husimi-distribution structure [22, 46, 47]. Furthermore, we determined qualitatively that the α -step size required to resolve an avoided crossing is correlated with the extent to which the participating states are localized in the chaotic and integrable regions of the phase space. An avoided crossing between two mixed states tends to be broader than that between a predominately regular state and a predominately chaotic state.

As the size of the uncoupled region is increased, the avoided crossings broaden and their density increases. This, in turn, increases the number of avoided-crossing clusters in which the participating energy-level curves do not fully exchange slopes. We showed numerically that such clusters of broad avoided crossings mix the Husimi structure between participating states rather than exchange them fully as in the sharp avoided crossings observed more frequently for uncoupled regions of small length. Such mixing tends to promote delocalization in the eigenstates as the coupling strength is increased. This causes a nontrivial modification in the aggregate Husimi structure as the coupling strength is varied, in contrast to the preservation of the aggregate Husimi structure characteristic of sharp avoided crossings. Consequently, as the length of the uncoupled region increases (so that there are more broad avoided crossings), one observes more and more mixing in the aggregate Husimi structure with increases in the coupling strength. This is a signature of the dynamics of the corresponding classical system, for which the chaotic portion of phase space increases with the size of the uncoupled region. Thus, the appearance of broad avoided crossings, eigenstate delocalization, and the mixing of Husimi structures seem to be signatures of chaos in the quantum system. Our numerical computations

suggest that the sharpness of avoided crossings is positively correlated with the extent to which the participating Husimi distributions are localized in different regions of phase space. Therefore, the dynamics of avoided crossings in quantum systems seems to be strongly related to the chaotic dynamics of their classical counterparts.

Acknowledgments

We thank Stephan De Bièvre, Mark Dykman, Jerry Marsden, Alex McCauley, Kevin Mitchell, Paul Parris, and Alex Silvius for useful discussions concerning this research. We also thank Alex Barnett and Mark Dykman for their commentary on early versions of this manuscript. TM acknowledges support from Caltech's Summer Undergraduate Research Fellowship (SURF) Program and the Richter Memorial Funds. MAP acknowledges support from the Gordon and Betty Moore Foundation through Caltech's Center for the Physics of Information.

Appendix I: The Hamiltonian Matrix

Let $\mathcal{H}_1 = \mathcal{H}_{part}$ be the Hilbert space for a free particle constrained to a ring of length $2 + L$ and $\mathcal{H}_2 = \mathcal{H}_{osc}$ be the Hilbert space for an uncoupled harmonic oscillator. Define $|n\rangle_1 = |\psi_n^{part}\rangle$ and E_n^1 , respectively, to be the n th eigenstate and corresponding n th eigenenergy for the particle. We calculate the coordinate-space projections $\{\psi_n^{part}(q)\}_{n=1}^{\infty}$ of $\{|n\rangle_1\}_{n=1}^{\infty}$ and their eigenenergies from the Schrödinger equation with periodic boundary conditions,

$$\begin{aligned} \frac{\partial^2}{\partial q^2} \psi_n^{part}(q) &= -E_n^1 \psi_n^{part}(q), \\ \psi_n^{part}(q + k(2 + L)) &= \psi_n^{part}(q), \quad k \in \mathbb{Z}. \end{aligned}$$

The (normalized) solutions are

$$\begin{aligned} \psi_n^{part}(q) &= \frac{1}{\sqrt{2 + L}} \exp \left\{ - \left(\frac{2\pi n i}{2 + L} \right) q \right\}, \\ E_n^1 &= \frac{4\pi^2 n^2}{(2 + L)^2}. \end{aligned} \tag{7}$$

The ground-state energy of the particle is $E_1^1 = 4\pi^2 / (2 + L)^2$. Define $|k\rangle_2 = |\psi_k^{osc}\rangle$ and E_k^2 to be the k th eigenstate and corresponding k th eigenenergy of the oscillator. Here, $E_k^2 = k + 1/2$, so that $E_0^2 = 1/2$ is the ground-state energy [12].

Using the operator definitions (5), we write

$$a^\dagger = \frac{1}{\sqrt{2}} (\Phi - i\Pi), \quad a = \frac{1}{\sqrt{2}} (\Phi + i\Pi),$$

which are the creation and annihilation operators, respectively, for the harmonic oscillator [12, 37]. The Hamiltonian (6) becomes

$$H = \left(a^\dagger a + \frac{1}{2} \right) - \frac{p^2}{2} - \frac{\alpha}{\sqrt{2}} (a^\dagger + a) \chi(q). \tag{8}$$

The matrix representation of (8) in the uncoupled basis $|n\rangle_1 \otimes |k\rangle_2$ [with integer indices $n \in [1, \infty)$ and $k \in [0, \infty)$] is

$$\mathbf{H} = \mathbf{E}_1 \otimes \mathbb{I} + \mathbb{I} \otimes \mathbf{E}_2 - \alpha \mathbf{W}_1 \otimes \mathbf{W}_2, \tag{9}$$

where \mathbb{I} is the identity matrix and

$$\begin{aligned} (\mathbf{E}_1)_{nn'} &= \left\langle n \left| \frac{-p^2}{2} \right| n' \right\rangle_1, & (\mathbf{E}_2)_{kk'} &= \left\langle k \left| \left(a^\dagger a + \frac{1}{2} \right) \right| k' \right\rangle_2, \\ (\mathbf{W}_1)_{nn'} &= \langle n | \chi(q) | n' \rangle_1, & (\mathbf{W}_2)_{kk'} &= \left\langle k \left| \frac{1}{\sqrt{2}} (a^\dagger + a) \right| k' \right\rangle_2. \end{aligned}$$

By the definition of the uncoupled basis,

$$(\mathbf{E}_1)_{nn'} = \frac{4\pi^2 n^2}{(2+L)^2} \delta_{nn'} , \quad (\mathbf{E}_2)_{kk'} = \left(k + \frac{1}{2} \right) \delta_{kk'} . \quad (10)$$

Additionally, the coordinate-space projections for the free particle eigenstates yield

$$(\mathbf{W}_1)_{nn'} = \int_0^{2+L} \psi_n^{part}(q)^* \psi_{n'}^{part}(q) \chi(q) dq = \int_0^2 \psi_n^{part}(q)^* \psi_{n'}^{part}(q) dq .$$

Hence, with Eq. (7), we obtain

$$(\mathbf{W}_1)_{nn'} = \begin{cases} \frac{1}{2\pi(n-n')} \left(-i + ie^{\frac{4\pi i(n-n')}{2+L}} \right) & \text{if } n \neq n', \\ \frac{2}{2+L} & \text{if } n = n' . \end{cases} \quad (11)$$

Finally, the creation/annihilation operator identities

$$a^\dagger |k\rangle_2 = \sqrt{k+1} |k+1\rangle_2 , \quad a|k\rangle_2 = \sqrt{k} |k-1\rangle_2 \quad (12)$$

yield

$$(\mathbf{W}_2)_{kk'} = \frac{1}{\sqrt{2}} \left(\sqrt{k'+1} \delta_{k,k'+1} + \sqrt{k'} \delta_{k,k'-1} \right) . \quad (13)$$

Appendix II: The Husimi Distribution

The Husimi distribution $H_\psi(\bar{p}, \bar{q}, \bar{\Phi}, \bar{\Pi})$ of a state $|\psi\rangle$ of the two-dimensional quantum mechanical system (6) is

$$H_\psi(\bar{p}, \bar{q}, \bar{\Phi}, \bar{\Pi}) = N |\langle \psi_{(\bar{p}, \bar{q}, \bar{\Phi}, \bar{\Pi})} | \psi \rangle|^2 , \quad (14)$$

where $|\psi_{(\bar{p}, \bar{q}, \bar{\Phi}, \bar{\Pi})}\rangle$ is a coherent state localized around $(\bar{p}, \bar{q}, \bar{\Phi}, \bar{\Pi})$ and N is a normalization constant. We construct a coherent state for the coupled system as the product

$$|\psi_{(\bar{p}, \bar{q}, \bar{\Phi}, \bar{\Pi})}\rangle = |\psi_{(\bar{p}, \bar{q})}\rangle_1 \otimes |\psi_{(\bar{\Phi}, \bar{\Pi})}\rangle_2 , \quad (15)$$

where $|\psi_{(\bar{p}, \bar{q})}\rangle_1$ is the coherent state for the uncoupled particle and $|\psi_{(\bar{\Phi}, \bar{\Pi})}\rangle_2$ is the coherent state for the uncoupled harmonic oscillator. The latter is given by [12]

$$|\psi_{(\bar{\Phi}, \bar{\Pi})}\rangle_2 = e^{-\frac{1}{2}(\bar{\Phi}^2 + \bar{\Pi}^2)} \sum_{k=0}^{\infty} \frac{(\bar{\Phi} + i\bar{\Pi})^k}{\sqrt{k!}} |k\rangle_2 . \quad (16)$$

Because the uncoupled particle system is $(2+L)$ -periodic in q and $p \in \mathbb{R}$, the phase space is cylindrical. We use the procedure of Spina and Skodje [41] to define $|\psi_{(\bar{p}, \bar{q}, \bar{\Phi}, \bar{\Pi})}\rangle$ for this topology. We require the coherent state $|\psi_{(\bar{p}, \bar{q})}\rangle_1$ to satisfy

$$\langle q | \psi_{(\bar{p}, \bar{q})} \rangle_1 = \langle q + k(2+L) | \psi_{(\bar{p}, \bar{q})} \rangle_1 , \quad k \in \mathbb{Z} . \quad (17)$$

One can construct the coherent states $|\psi_{(\bar{p}, \bar{q})}\rangle_1$ from the Euclidean coherent states $|\tilde{\psi}_{(\bar{p}, \bar{q})}\rangle_1$ (which are Gaussian wavefunctions) by wrapping them around the cylinder and summing overlapping portions. This yields

$$\langle q | \psi_{(\bar{p}, \bar{q})} \rangle_1 = C^{\frac{1}{2}} \sum_{k=-\infty}^{\infty} \langle q + k(2+L) | \tilde{\psi}_{(\bar{p}, \bar{q})} \rangle_1 , \quad (18)$$

which satisfies (17) and converges because $\langle q + k(2+L) | \tilde{\psi}_{(\bar{p}, \bar{q})} \rangle_1$ is Gaussian. In Eq. (18), the quantity C is a normalization constant to be determined by the condition $\langle \psi_{(\bar{p}, \bar{q})} | \psi_{(\bar{p}, \bar{q})} \rangle_1 = 1$.

The projection of $|\psi_{(\bar{p},\bar{q})}\rangle_1$ onto the uncoupled-particle basis $\{|n\rangle_1\}_{n=1}^\infty$ is

$$\langle n|\psi_{(\bar{p},\bar{q})}\rangle_1 = \int_0^{2+L} \langle n|q\rangle_1 \langle q|\psi_{(\bar{p},\bar{q})}\rangle_1 dq = C^{\frac{1}{2}} \sum_{k=-\infty}^{\infty} \int_0^{2+L} \langle n|q+k(2+L)\rangle_1 \langle q+k(2+L)|\tilde{\psi}_{(\bar{p},\bar{q})}\rangle_1 dq.$$

Using the $(2+L)$ periodicity of $\psi_n^{part}(q) = \langle q|n\rangle_1$ and Eq. (7), we obtain

$$\langle n|\psi_{(\bar{p},\bar{q})}\rangle_1 = \int_{-\infty}^{\infty} \langle n|q\rangle_1 \langle q|\tilde{\psi}_{(\bar{p},\bar{q})}\rangle_1 dq. \quad (19)$$

The coordinate-space projection of the Euclidean coherent state is

$$\langle q|\tilde{\psi}_{(\bar{p},\bar{q})}\rangle_1 = \left(\frac{1}{\pi}\right)^{\frac{1}{4}} \exp\left(-\frac{1}{2}(q-\bar{q})^2 + i\bar{p}\left(q-\frac{\bar{q}}{2}\right)\right). \quad (20)$$

Using the above with the expression for $\psi_n^{part}(q) = \langle q|n\rangle_1$ in (7), we evaluate (19) and obtain

$$\langle n|\psi_{(\bar{p},\bar{q})}\rangle_1 = C^{\frac{1}{2}} \left(\frac{1}{2}\right)^{\frac{1}{4}} \exp\left(-\frac{1}{2}(n-\bar{p})^2 - i\bar{q}\left(n-\frac{\bar{p}}{2}\right)\right). \quad (21)$$

With the normalization condition $\langle\psi_{(\bar{p},\bar{q})}|\psi_{(\bar{p},\bar{q})}\rangle_1 = 1$, we determine from (21) that

$$C(\bar{p}) = \sqrt{\pi} \sum_{n=-\infty}^{\infty} e^{-(n-\bar{p})^2}, \quad (22)$$

where we have emphasized the dependence of C on \bar{p} by writing $C = C(\bar{p})$.

Thus, if a state $|\psi\rangle$ is expressed in the uncoupled basis $|n\rangle_1 \otimes |k\rangle_2$ as $|\psi\rangle = \sum_{n=1,k=0}^{\infty} a_{nk} |n\rangle_1 \otimes |k\rangle_2$, we obtain from (14), (16), and (21) that

$$H_\psi(\bar{p},\bar{q},\bar{\Phi},\bar{\Pi}) = \frac{C(\bar{p})}{\sqrt{2}} \left| \sum_{n=1,k=0}^{\infty} a_{nk}^* \frac{(\bar{\Phi} + i\bar{\Pi})^k}{\sqrt{k!}} \times \exp\left(-\frac{1}{2}[\bar{\Phi}^2 + \bar{\Pi}^2 + (n-\bar{p})^2] - i\bar{q}\left(n-\frac{\bar{p}}{2}\right)\right) \right|^2. \quad (23)$$

In practice, we truncate the sum in Eq. (23) in order to compute the Husimi distribution for eigenstates calculated using a truncated Hamiltonian matrix for (6). To compare Husimi distributions with classical Poincaré surface of sections, we take $\bar{q} = 1$ and $\bar{p} = (2E - \bar{\Phi}^2 - \bar{\Pi}^2 + 2\alpha\bar{\Phi})^{1/2}$ for an eigenstate of energy E . The first condition arises from a convention in choosing the Poincaré SOS for the classical system [14], and the second arises as a slice along the classical energy shell.

[1] M. F. Anderson, A. Kaplan, T. Grünzweig, and N. Davidson. Decay of quantum correlations in atom optics billiards with chaotic and mixed dynamics. *quant-ph/0404118*, 2004.

[2] D. V. Anosov and Ya. G. Sinai. Some smooth ergodic systems. *Russian Mathematical Surveys*, 22:103–167, 1967.

[3] V. I. Arnold. Proof of A. N. Kolmogorov’s theorem on the preservation of quasiperiodic motions under small perturbations of the Hamiltonian. *Russian Mathematical Surveys*, 18(5):9–36, 1963.

[4] V. I. Arnold. Small divisor problems in classical and celestial mechanics. *Russian Mathematical Surveys*, 18(6):85–192, 1963.

[5] A. Backer, S. Furstberger, and R. Schubert. Poincaré Husimi representation of eigenstates in quantum billiards. *Physical Review E*, 70(3):036204, 2004.

[6] A. H. Barnett and T. Betcke. Quantum mushroom billiards. *nlin.CD/0611059*, 2006.

[7] M. V. Berry. Regularity and chaos in classical mechanics, illustrated by three deformations of a circular billiard. *European Journal of Physics*, 2:91–102, 1981.

[8] L. A. Bunimovich. Mushrooms and other billiards with divided phase space. *Chaos*, 11(4):802–808, 2001.

[9] A. O. Caldeira and A. J. Leggett. Quantum tunnelling in a dissipative system. *Annals of Physics*, 149(2):374–456, 1983.

[10] S.-J. Chang and G. Perez. Classical and quantum eigenstates of a kicked rotor. *Chinese Journal of Physics*, 30(4):479–495, 1992.

[11] S.-J. Chang and M. Stuller. The quantum kicked rotor revisited. *Chinese Journal of Physics*, 35(4):469–479, 1997.

- [12] C. Cohen-Tannoudji, B. Diu, and F. Laloë. *Quantum Mechanics*, volume Vol. 1. John Wiley & Sons, New York, NY, 1977.
- [13] P. Cvitanović, R. Artuso, R. Mainieri, G. Tanner, and G. Vattay. *Chaos: Classical and Quantum*, volume 11. Niels Bohr Institute, Copenhagen, July 2005. ChaosBook.org.
- [14] S. De Bièvre, P. E. Parris, and A. Silvius. Chaotic dynamics of a free particle interacting linearly with a harmonic oscillator. *Physica D*, 208(1-2):96–114, 2005.
- [15] R. P. Feynman. Slow electrons in a polar crystal. *Physical Review*, 97(3):660–665, 1955.
- [16] N. Friedman, A. Kaplan, D. Carasso, and N. Davidson. Observation of chaotic and regular dynamics in atom-optics billiards. *Physical Review Letters*, 86(8):1518–1521, 2001.
- [17] H. Froölich. Electrons in lattice fields. *Advances in Physics*, 3(11):325–361, 1954.
- [18] R. González-Férez and J. S. Dehesa. Characterization of atomic avoided crossings by means of Fisher's information. *The European Physical Journal D*, 32:39–43, 2005.
- [19] M. C. Gutzwiller. *Chaos in Classical and Quantum Mechanics*. Number 1 in Interdisciplinary Applied Mathematics. Springer-Verlag, New York, NY, 1990.
- [20] M. C. Gutzwiller. Quantum chaos. *Scientific American*, 266:78–84, 1992.
- [21] F. Haake. *Quantum Signatures of Chaos*. Springer Series in Synergetics. Springer-Verlag, Berlin, Germany, 2nd edition, 2001.
- [22] B. P. Holder and L. E. Reichl. Avoided crossings in driven systems. *Physical Review A (Atomic, Molecular, and Optical Physics)*, 72(4):043408, 2005.
- [23] T. Holstein. Studies of polaron motion. part i. the molecular-crystal model. *Annals of Physics*, 8(3):325–342, 1959.
- [24] T. Holstein. Studies of polaron motion. part ii. the “small” polaron. *Annals of Physics*, 8(3):343–389, 1959.
- [25] D. W. Hone, R. Ketzmerick, and W. Kohn. Time-dependent Floquet theory and absence of an adiabatic limit. *Physical Review A*, 56(5):4045–4054, 1997.
- [26] V. M. Kenkre and D. K. Campbell. Self-trapping on a dimer–time-dependent solutions of a discrete nonlinear Schrödinger-equation. *Physical Review B*, 34(7):4959–4961, 1986.
- [27] V. M. Kenkre and L. Giuggioli. Study of some approximation schemes in the spin-boson problem. *Chemical Physics*, 296(2-3):135–148, 2004.
- [28] A. N. Kolmogorov. On conservation of conditionally periodic motions under small perturbations of the Hamiltonian. *Dokl. Akad. Nauk. SSSR*, 98:527–530, 1954.
- [29] A. Kudrolli, V. Kidambi, and S. Sridhar. Experimental studies of chaos and localization in quantum wave functions. *Physical Review Letters*, 75(5):822–825, July 1995.
- [30] C. M. Marcus, A. J. Rimberg, R. M. Westervelt, P. F. Hopkins, and A. C. Gossard. Conductance fluctuations and chaotic scattering in ballistic microstructures. *Physical Review Letters*, 69(3):506–509, July 1992.
- [31] J. Moser. On invariant curves of area-preserving mappings of an annulus. *Nachr. Akad. Wiss. Göttingen Math. Phys. Kl.*, 2:1–20, 1962.
- [32] L. Perotti. Quantum double pendulum: Study of an autonomous classically chaotic quantum system. *Physical Review E*, 70(6):066218, 2004.
- [33] M. A. Porter and S. Lancel. Mushroom billiards. *Notices of the American Mathematical Society*, 53(3):334–337, 2006.
- [34] B. Ramachandran and K. G. Kay. The influence of classical resonances on quantum energy levels. *Journal of Chemical Physics*, 99(5):3659–3668, 1993.
- [35] L. E. Reichl. *The Transition to Chaos: Conservative Classical Systems and Quantum Manifestations*. Springer-Verlag, New York, NY, 2nd edition, 2004.
- [36] N. Saitô, H. Hirooka, J. Ford, F. Vivaldi, and G. H. Walker. Numerical study of billiard motion in an annulus bounded by non-concentric circles. *Physica D*, 5:273–286, 1982.
- [37] R. Shankar. *Principles of Quantum Mechanics*. Plenum Press, New York, NY, 2nd edition, 1994.
- [38] A. A. Silvius, P. E. Parris, and S. De Bièvre. Adiabatic-nonadiabatic transition in the diffusive Hamiltonian dynamics of a classical Holstein polaron. *Physical Review B*, 73(1):014304, 2006.
- [39] Ya. G. Sinai. On the foundation of the ergodic hypothesis for a dynamical system of statistical mechanics. *Dokl. Akad. Nauk. SSSR*, 153:1261–1264, 1963.
- [40] S. Smale. Differentiable dynamical systems. *Bulletin of the American Mathematical Society*, 73:747–817, 1967.
- [41] A. Spina and R. T. Skodje. The phase-space hydrodynamic model for the quantum standard map. *Computer Physics Communications*, 63:279–305, 1991.
- [42] J. Stein and H. J. Stöckmann. Experimental-determination of billiard wave-functions. *Physical Review Letters*, 68(19):2867–2870, 1992.
- [43] H. J. Stöckmann and J. Stein. Quantum chaos in billiards studied by microwave-absorption. *Physical Review Letters*, 64(19):2215–2218, 1990.
- [44] A. Sugita. Moments of generalized Husimi distributions and complexity of many-body quantum states. *Journal of Physics A: Mathematical and General*, 36(34):9081–9104, 2003.
- [45] A. Sugita and H. Aiba. Second moment of the Husimi distribution as a measure of complexity of quantum states. *Phys. Rev. E*, 65(3):036205, Feb 2002.
- [46] T. Timberlake and L. E. Reichl. Changes in floquet-state structure at avoided crossings: Delocalization and harmonic generation. *Phys. Rev. A*, 59(4):2886–2893, Apr 1999.
- [47] J. von Neumann and E. Wigner. On the behavior of eigenvalues in adiabatic processes. In Robert S. Knox and Albert Gold, editors, *Symmetry in the Solid State*. W. A. Benjamin, Inc., New York, NY, 1964. [English translation of “Uber das Verhalten von Eigenwerten bei Adiabatischen Prozessen,” *Physikalische Zeitschrift* **30**, 467–470 (1929).].

[48] J. Wiersig. Formation of long-lived, scarlike modes near avoided resonance crossings in optical microcavities. *Physical Review Letters*, 97:253901, 2006.

[49] C. Zhang, J. Liu, M. G. Raizen, and Q. Niu. Quantum chaos of Bogoliubov waves for a Bose-Einstein condensate in stadium billiards. *Physical Review Letters*, 93:074101, 2004.

[50] W.-M. Zhang, D. H. Feng, J.-M. Yuan, and S.-J. Wang. Integrability and nonintegrability of quantum systems: Quantum integrability and dynamical symmetry. *Physical Review A*, 40:438447, 1989.

[51] W.-M. Zhang, C. C. Martens, D. H. Feng, and J.-M. Yuan. Dynamical symmetry breaking and quantum nonintegrability. *Physical Review Letters*, 61:2167–2170, 1988.

[52] Formally, $|\psi_{k+1}^{part}\rangle \otimes |\psi_l^{osc}\rangle$ is an element of the tensor product space $\mathcal{H}_{part} \otimes \mathcal{H}_{osc}$, where \mathcal{H}_{part} and \mathcal{H}_{osc} are the particle and oscillator Hilbert spaces, respectively. One can also think of $|\psi_{k+1}^{part}\rangle \otimes |\psi_l^{osc}\rangle$ in terms of the coordinate-space wavefunction $\psi_{k+1}^{part}(q)\psi_l^{osc}(\Phi) = \langle q, \Phi | \{|\psi_{k+1}^{part}\rangle \otimes |\psi_l^{osc}\rangle\} \rangle$ [12].

[53] A Hamiltonian H is invariant under a symmetry transformation S if $[H, S]=0$.

[54] We use the term “isolated cluster” to designate a sequence of nearby avoided crossings whose participating energy levels are nearly unaffected by other levels in their “incoming” (as a function of α) and outgoing regions.

Energy Levels for a System with $L=20$

